An ultrashort pulse ultra-violet radiation undulator source driven by a laser plasma wakefield accelerator

M. P. Anania,[1,2] E. Brunetti,[1] S. M. Wiggins,[1] D. W. Grant,[1] G. H. Welsh,[1] R. C. Issac,[1] S. Cipiccia,[1] R. P. Shanks,[1] G. G. Manahan,[1] C. Aniculaesei,[1] S. B. van der Geer,[3] M. J. de Loos,[3] M. W. Poole,[4] B. J. A. Shepherd,[4] J. A. Clarke,[4] W. A. Gillespie,[5] A. M. MacLeod,[6] and D. A. Jaroszynski[1,a)]

[1]*SUPA, Department of Physics, University of Strathclyde, Glasgow G4 0NG, United Kingdom*
[2]*INFN, Laboratori Nazionali di Frascati, I-00044 Frascati, Italy*
[3]*Pulsar Physics, Burghstraat 47, 5614 BC Eindhoven, The Netherlands*
[4]*ASTeC, STFC, Daresbury Laboratory, Warrington WA4 4AD, United Kingdom*
[5]*SUPA, School of Engineering, Physics and Mathematics, University of Dundee, Dundee DD1 4HN, United Kingdom*
[6]*School of Computing and Creative Technologies, University of Abertay Dundee, Dundee DD1 1HG, United Kingdom*

(Received 14 May 2014; accepted 23 June 2014; published online 1 July 2014)

Narrow band undulator radiation tuneable over the wavelength range of 150–260 nm has been produced by short electron bunches from a 2 mm long laser plasma wakefield accelerator based on a 20 TW femtosecond laser system. The number of photons measured is up to 9×10^6 per shot for a 100 period undulator, with a mean peak brilliance of 1×10^{18} photons/s/mrad^2/mm^2/0.1% bandwidth. Simulations estimate that the driving electron bunch r.m.s. duration is as short as 3 fs when the electron beam has energy of 120–130 MeV with the radiation pulse duration in the range of 50–100 fs. [http://dx.doi.org/10.1063/1.4886997]

The laser wakefield accelerator (LWFA) utilizes the strong electrostatic forces of femtosecond laser-driven plasma density waves as an accelerating medium to support large accelerating gradients of more than 100 MeV/mm.[1,2] It has been proposed as a compact driver of undulator radiation,[3–5] which has recently been demonstrated initially in the visible[6] and then in the extreme ultra-violet[7] spectral range. The high peak current, quasi-monoenergetic, and ultrashort electron bunches ensure an inherently high peak brilliance source of undulator radiation[8] tuneable over a wide spectral range.

In this Letter, we present a demonstration of a source of LWFA-driven narrow bandwidth undulator radiation in the vacuum ultra-violet (VUV) spectral range. LWFAs could ultimately serve the large user communities of next-generation synchrotron and free-electron laser (FEL) light sources at shorter wavelengths.[8,9] However, of immediate interest in the VUV range are applications in ultrafast spectroscopy[10,11] of photo- and biochemical processes, including femtochemistry[12] and femtobiology,[13] that require a temporal resolution of 10 fs or less. The prospect of a LWFA-driven VUV undulator radiation source for such applications is demonstrated by simulations of our electron beam transport, carried out using the General Particle Tracer (GPT) code[14] and presented in Fig. 1 (the beam line is described in more detail later). These show that an r.m.s. electron bunch duration as low as 2.7 fs is predicted for the undulator radiation driver. This would strongly correlate with the subsequent radiation pulse duration making it attractive for ultrafast studies. Furthermore, sufficient bunch charge ($\geq$3 pC) allows the peak current to reach kA levels, where single-pass high-gain FEL may become feasible.[15]

The Advanced Laser-Plasma High-energy Accelerators towards X-rays (ALPHA-X) accelerator beam line,[3] as shown in Fig. 2(a), has been used for the investigations presented here. A Ti:sapphire laser pulse (central wavelength $\lambda_0 = 800$ nm, full-width at half-maximum duration = 36 fs, and peak intensity $= 2 \times 10^{18}$ W/cm^2) is focused to a 20 μm waist (radius at $1/e^2$) at the leading edge of a 2 mm diameter helium gas jet to form a relativistic self-guided plasma channel with a relativistic plasma wavelength $\lambda_p = 2\pi c/\omega_p \approx 10.6\,\mu$m, where c is the speed of light, $\omega_p = (n_e e^2/\varepsilon_0 m_e)^{1/2}$, n_e is the electron density, ε_0 is the permittivity of free space, and e and m_e

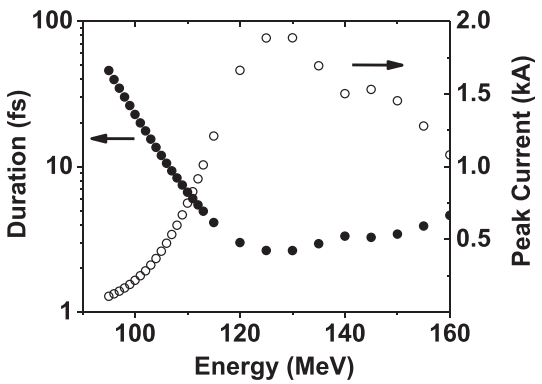

FIG. 1. Simulations showing the dependence on the electron energy (given a fixed magnetic transport system) of the electron r.m.s. bunch duration and peak current at the undulator entrance. Simulation initial bunch parameters: 5% r.m.s. energy spread, 5 pC charge, 1.75 mrad half-angle divergence, 1 μm r.m.s. radius, 0.9 fs r.m.s. duration.

a)Author to whom correspondence should be addressed. Electronic mail: d.a.jaroszynski@strath.ac.uk

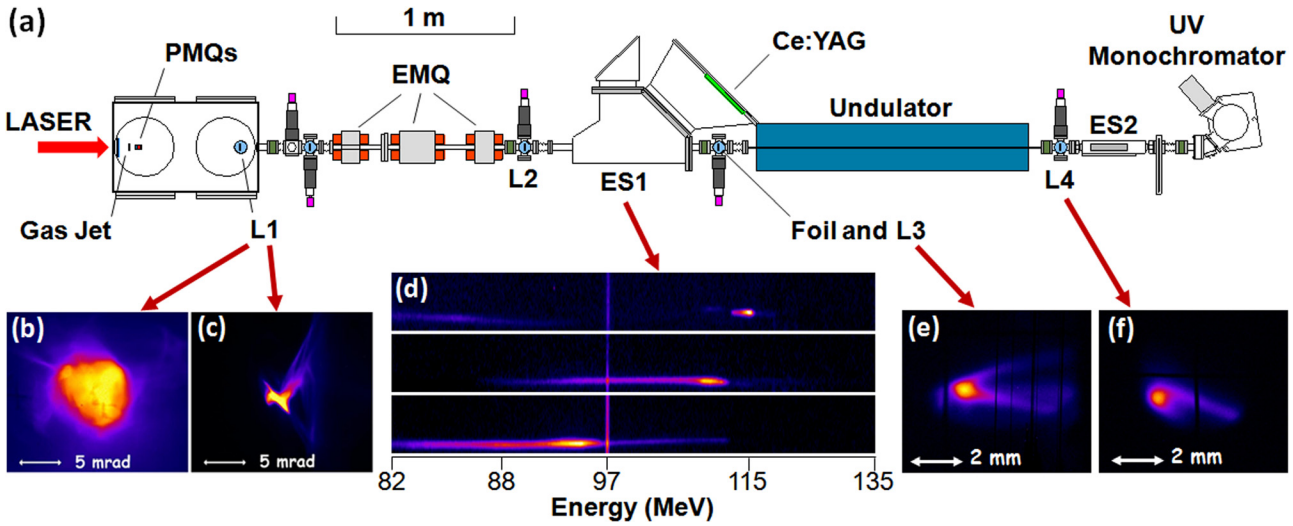

FIG. 2. (a) Plan view of the ALPHA-X LWFA beam line, false color images of the electron beam profile at (b) L1 without PMQs, (c) L1 with PMQs in-line, (e) L3 and (f) L4 and (d) three examples of ES1 spectra with main peak central energy and charge of 115, 109, 95 MeV and 0.4, 0.8, 1.3 pC, respectively.

are the electron charge and mass, respectively. The normalized laser vector potential, initially, $a_0 = eA/m_e c^2 \approx 1$, where A is the vector potential, grows to $a_0 > 3$ due to non-linear self-focusing and photon acceleration,[16] which results in a trailing evacuated plasma bubble into which electrons are injected from the background plasma.

Electron beams exiting the accelerator are initially collimated using a triplet of miniature permanent magnet quadrupoles (PMQs).[17,18] The field gradient of each quadrupole is ~500 T/m, and the triplet entrance is 30 mm from the accelerator exit. A triplet of electromagnetic quadrupoles (EMQs) then focuses the beam through the undulator. The respective EMQ field gradients are 2.47 T/m, 2.20 T/m, and 2.47 T/m. The quadrupoles are set for optimal transport of 130 MeV energy electrons (Fig. 2), and, within ±10 MeV of this design energy, the simulated electron bunch duration at the undulator entrance is predicted to be ~3 fs (Fig. 1). Experimental measurements of the duration that detect transition radiation generated by the beam passing through a metal foil perturb the beam too strongly for simultaneous use with the undulator, however, other studies on ALPHA-X[19] and elsewhere[20] show that the duration of the electron beam within 1 m of the accelerator is ~1–2 fs, and this is the basis for the beam transport simulations. Beam profile monitors at positions L1, L2, L3, and L4 comprise phosphor Lanex screens and 12-bit charge-coupled device (CCD) cameras.

An imaging dipole magnetic electron spectrometer (ES1) provides strong focusing in the horizontal and vertical planes thus enabling excellent energy resolution (~0.5%–1.0%), which can be maintained over a wide energy range (83–196 MeV at the field strength of 0.52 T). Ce:YAG crystals positioned in the focal plane image electrons dispersed by the spectrometer magnetic field with the image captured on a 14-bit CCD camera. The electron beam dump after the undulator is a simple permanent dipole bending magnet that acts as a rudimentary compact electron spectrometer (ES2). This allows UV radiation and electron spectra to be captured simultaneously. The on-axis magnetic field strength of ES2 is 0.75 T suitable for electrons in the range of 20–250 MeV to be imaged on a Lanex screen by a 12-bit CCD camera. All Lanex and Ce:YAG screens (except L1) have been cross-calibrated against imaging plate measurements to determine the absolute electron beam charge.[21]

The undulator (length 1.5 m, $N_u = 100$ periods, and $\lambda_u = 15$ mm) has a slotted pole planar design and the adjustable pole gap is set at 8.0 mm for these experiments (vacuum tube inner diameter is 6 mm). This gives a peak on-axis magnetic field strength $B_u = 0.27$ T and undulator deflection parameter $K = 0.38$. The slotted pole design of the undulator features a 5 mm by 1 mm slot cut out of the central section of the magnets. This provides a radial focusing force for electrons of energy up to ~100 MeV. Full details are given elsewhere.[22] The distance from accelerator exit to undulator entrance is 3.52 m.

Undulator output radiation is detected using a vacuum scanning monochromator (with platinum-coated toroidal mirror and 300 lines/mm grating) and 16-bit CCD camera. The grating is positioned for a 344 nm detection bandwidth centred on 220 nm with a resolution of about 5 nm. Three elements attenuate the radiation signal: the toroidal mirror (peak reflectivity of 65%), the grating (peak efficiency of 25% at 150 nm), and finally the quantum efficiency of the camera (25% across the relevant spectral range). Laser light and plasma emission has been blocked by an aluminium foil (thickness 800 nm) positioned before the undulator at Lanex screen L3.

Removal of the PMQs enables the intrinsic divergence and profile of the electron beam to be observed on Lanex screen L1. The mean r.m.s. divergence is 3.5 mrad (Fig. 2(b)), which is reduced to 1 mrad (Fig. 2(c)) upon insertion of the PMQs, i.e., near collimation of the central part of the beam. The PMQs act as an energy bandpass filter, imparting large angle trajectories on electrons outside of their acceptance range. Hence, outlying swirls that are evident in the Lanex image are related to the low energy "tail" or pedestal of the electron beam. The main central part of the beam, comprising the higher energy quasi-monoenergetic "main peak" electron bunch, is the sole part of the beam that is preferentially transported through the undulator. Electron energy spectra obtained with ES1 (Fig. 2(d)) illustrate the

broad range of beam energies from the accelerator that are due to laser and plasma density fluctuations. Typically, ~30% of the charge is contained in the main high energy peak and ~70% in the (mainly) lower energy pedestal. At ES1, the main peak has a mean central energy of 104 ± 9 MeV, with a 5% relative energy spread, and contains a mean charge of (1.1 ± 0.8) pC.

The L3 and L4 images (Figs. 2(e) and 2(f), respectively, before and after the undulator) indicate reasonable focusing and transport of the main peak electrons through the undulator. At L3, the mean r.m.s. width is $580 \times 510\ \mu$m (smallest $240 \times 290\ \mu$m). At L4, the mean width is $800 \times 710\ \mu$m (smallest $360 \times 400\ \mu$m). The GPT transport simulations also predict sub-mm beam widths at the screen positions but the energy-dependence inherent in transport and the fact that the electron beam energy is not captured simultaneously with either Lanex image makes direct comparison with the experimental mean values difficult. Further simulations estimate an acceptable focal waist of less than 150 μm close to the centre of the undulator[21] when L3 and L4 widths are in the range of 200–400 μm, and we estimate that this condition has been satisfied experimentally for at least 25% of all shots. An estimated beta function of 0.2 m indicates that matching to the undulator length (1.5 m) is typically not optimal. The mean measured charge, averaged over the 10 shots of highest charge, is 4.5 pC at L3 and 2.3 pC at L4, respectively. However, ES2 spectra (Fig. 3) contain a lower mean charge of (0.8 ± 0.4) pC but without a pedestal. Therefore, we conclude that beam loss along the undulator is dominated by the loss of low energy pedestal electrons and that beam loss for the "main peak" electrons is low (<30%). The lower charge limits the peak current at the undulator entrance to ~0.35 kA, according to Fig. 1.

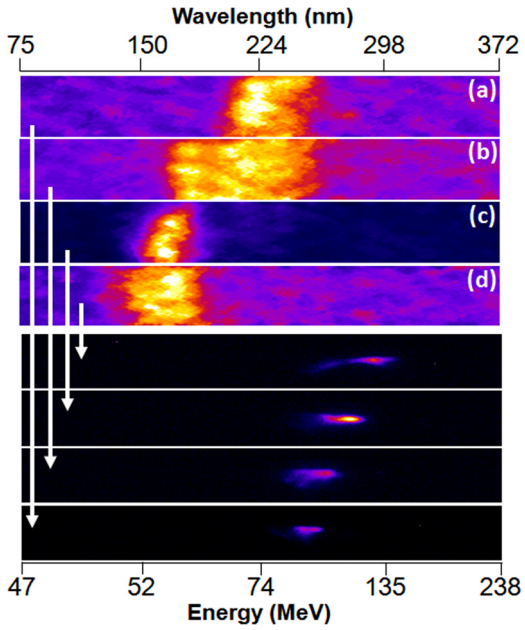

FIG. 3. False color images of four unprocessed undulator radiation spectra with corresponding ES2 electron spectra indicated. Respective values for number of detected photons (after processing for toroidal mirror, grating, and camera response), electron beam charge, and central energy are (a) 1.2×10^6, 0.9 pC, and 92 MeV, (b) 7.7×10^6, 1.6 pC, and 95 MeV, (c) 6.1×10^6, 2.0 pC, and 108 MeV and (d) 4.0×10^6, 1.3 pC, and 122 MeV.

Examples of measured radiation spectra and their corresponding ES2 electron spectra are shown in Fig. 3. No radiation is detected in the absence of an electron beam propagating through the undulator, while the classic radiation wavelength dependence on electron energy (wavelength scaling inversely with the square of the energy)[8] is obtained. The ES2 beam dump demonstrated its value as a crude electron spectrometer with a mean measured central energy of (102 ± 8) MeV that agrees well with the expected mean energy of (99 ± 4) MeV, obtained from the mean radiation wavelength λ_r of (216 ± 16) nm. This electron energy is less than the 130 MeV design energy such that, from Fig. 1, the mean electron bunch duration at the undulator entrance is estimated to be 28 fs. The mean spectral bandwidth of the radiation is (69 ± 11) nm or (32 ± 7) %, decreasing to as low as 16%, which is related to the electron beam properties[23] such that $(\delta\lambda_r/\lambda_r)^2 \approx (2\sigma_\gamma/\gamma)^2 + (\theta^2\gamma^2)^2$, where σ_γ/γ is the relative energy spread, θ is the divergence, and the natural bandwidth $1/N_u = 1\%$ has been neglected. Applying an electron beam divergence of 0.8 mrad from the L4 data, the dominant contribution to the spectral bandwidth is seen to be the electron energy spread (~15%, in agreement with deconvoluted ES2 spectra). This is a larger spread than that measured for the main peak at ES1, which indicates that a significant proportion of the radiation may originate from the pedestal electrons that are lost in transit through the undulator.

The scaling of the number of detected photons with electron charge (taking into account the attenuation by the grating, etc.), as shown in Fig. 4(a), confirms that the undulator radiation emission is incoherent spontaneous synchrotron-like radiation. A non-linear scaling would have

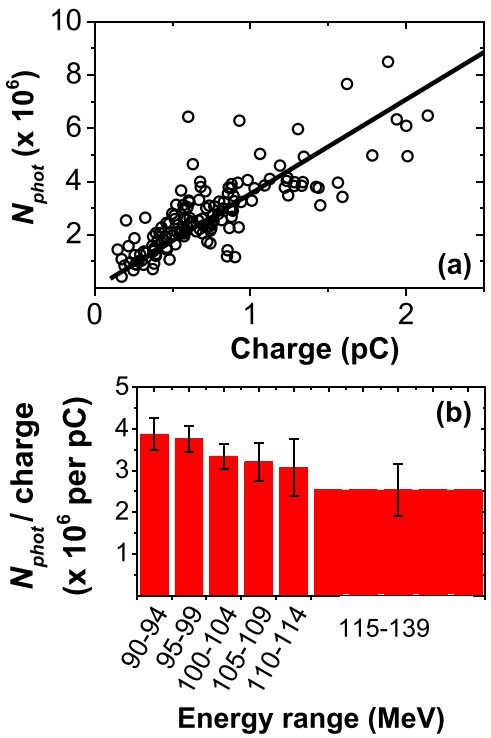

FIG. 4. (a) Dependence of the number of photons N_{phot} on the electron beam charge where the solid line is a linear best-fit and (b) average N_{phot} per unit charge as a function of the electron energy binned at 5 MeV intervals except in the high energy range (115–139 MeV), where eight shots have been binned together. The total dataset comprises 145 shots.

been evidence of coherent FEL emission. A significant increase in the efficiency of photon production has been obtained at lower electron energy, as shown in Fig. 4(b). This is relatively far from the nominal optimal transport energy (130 MeV) and can be attributed to the ever greater focusing effect imparted on electrons of less than 100 MeV energy by the slotted undulator field. Note that the total number of detected photons is up to 9×10^6, which is ~1–2 orders of magnitude greater than that obtained in the two previous experiments.[6,7]

In summary, a bright tunable source of ultrashort pulse UV radiation has been demonstrated. The estimated mean number of photons per shot per mrad^2 per 0.1% bandwidth is 2200 with a mean energy of 2.6 pJ and mean peak brilliance of 1×10^{18} photons/s/mrad^2/mm^2/0.1% bandwidth (based on the measured radiation divergence of 2 mrad, estimated source diameter of 300 μm, and mean r.m.s. duration of 100 fs). This is higher than the estimated values of 6.5×10^{16} and 1.3×10^{17} photons/s/mrad^2/mm^2/0.1% bandwidth, respectively, obtained in the visible[6] and extreme UV[7] spectral ranges where larger photon beam size estimates were applied. In terms of laser-driven light sources, higher peak brilliance of $\sim 1 \times 10^{19}$ photons/s/mrad^2/mm^2/0.1% bandwidth is reported for an X-ray LWFA-Compton source (100 TW laser, 30 fs radiation pulse duration, and 50% radiation spectral bandwidth).[24] Our relatively long radiation pulse duration is a sum of the mean electron duration (28 fs simulated) and mean radiation slippage duration ($N_u \lambda_r / c = 72$ fs). At the shortest observed wavelength of 150 nm, the radiation slippage duration is 50 fs. For shots predicted to have the shortest electron bunch lengths (down to 3 fs from Fig. 1), the radiation pulse duration could reduce to ~10 fs for user applications at the expense of fewer undulator periods and even shorter wavelength radiation, for example, $N_u = 40$ and $\lambda_r = 80$ nm. Furthermore, the average brilliance is limited by our pulse repetition frequency (PRF) of 1 Hz due to vacuum pump gas loading, but the current technological upper limit is the laser system PRF of 10 Hz. Future advances in repetition rates of gas delivery[25] and high-power femtosecond laser systems[26] will enable the average brilliance to be greatly improved.

Electron beam transport that minimizes bunch lengthening would reduce the mean electron bunch duration in the undulator and, hence, the radiation pulse duration from shot-to-shot. This would entail tuning the quadrupole settings (PMQ axial spacings, EMQ field strengths) for the given electron beam energy (dependent on laser and accelerator parameters). The desired wavelength for any particular application governs the precise experimental setup. A strong motivation for minimizing bunch duration, besides improving the temporal resolution for ultrafast spectroscopy, is the opportunity to improve the coherence properties of the radiation. Very short bunches or even those with a rapid longitudinal structural variation, such as a sharp rise or fall time, will have finite Fourier components at the radiation wavelength λ that could drive coherent spontaneous emission (CSE)[27] and, ultimately, FEL operation if other electron beam criteria (low energy spread and emittance) are satisfied. Longer wavelength systems have demonstrated that bunch rise times $\sim 10\lambda/c$, where c is the speed of light in vacuum, are sufficiently rapid to seed self-amplified coherent spontaneous emission (SACSE) in FELs.[28,29] At $\lambda = 150$ nm, for example, this corresponds to a threshold rise time ~5 fs. For our beam line setup as modelled in Fig. 1, the SACSE seeding condition is close to being fulfilled around the resonant electron energy of ≈120 MeV, however, the energy spread reported here would be around one order of magnitude too large for SACSE to occur (the slice energy spread may be lower). Clearly, as λ decreases, the requirement for a resonant Fourier beam component will be more difficult to satisfy, but very short (femtosecond) sub-structure has already been observed in LWFA electron beams.[30]

We acknowledge support of the U.K. EPSRC (Grant No. EP/J018171/1), the EC's LASERLAB-EUROPE (Grant Agreement No. 284464, Seventh Framework Programme), EuCARD-2 (Grant No. 312453, FP7) and the Extreme Light Infrastructure (ELI) European Project. We thank D. Clark and T. McCanny for technical support.

[1]T. Tajima and J. M. Dawson, Phys. Rev. Lett. **43**, 267 (1979).
[2]E. Esarey, C. B. Schroeder, and W. P. Leemans, Rev. Mod. Phys. **81**, 1229 (2009).
[3]D. A. Jaroszynski, R. Bingham, E. Brunetti, B. Ersfeld, J. Gallacher, B. van der Geer, R. Issac, S. P. Jamison, D. Jones, M. de Loos, A. Lyachev, V. Pavlov, A. Reitsma, Y. Saveliev, G. Vieux, and S. M. Wiggins, Philos. Trans. R. Soc., A **364**, 689 (2006).
[4]F. Gruener, S. Becker, U. Schramm, T. Eichner, M. Fuchs, R. Weingartner, D. Habs, J. Meyer-ter-Vehn, M. Geissler, M. Ferrario, L. Serafini, B. van der Geer, H. Backe, W. Lauth, and S. Reiche, Appl. Phys. B **86**, 431 (2007).
[5]C. B. Schroeder, W. M. Fawley, F. Gruener, M. Bakeman, K. Nakamura, K. E. Robinson, Cs. Toth, E. Esarey, and W. P. Leemans, AIP Conf. Proc. **1086**, 637 (2009).
[6]H.-P. Schlenvoigt, K. Haupt, A. Debus, F. Budde, O. Jäckel, S. Pfotenhauer, H. Schwoerer, E. G. Rohwer, J. G. Gallacher, E. Brunetti, R. P. Shanks, S. M. Wiggins, and D. A. Jaroszynski, Nat. Phys. **4**, 130 (2008).
[7]M. Fuchs, R. Weingartner, A. Popp, Zs. Major, S. Becker, J. Osterhoff, I. Cortrie, B. Zeitler, R. Hoerlein, G. D. Tsakiris, U. Schramm, T. P. Rowlands-Rees, S. M. Hooker, D. Habs, F. Krausz, S. Karsch, and F. Gruener, Nat. Phys. **5**, 826 (2009).
[8]P. Rebernik Ribic and G. Margaritondo, J. Phys. D: Appl. Phys. **45**, 213001 (2012).
[9]B. W. J. McNeil and N. R. Thompson, Nat. Photonics **4**, 814 (2010).
[10]G. C. Walker, W. Jarzeba, T. J. Kang, A. E. Johnson, and P. E. Barbara, J. Opt. Soc. Am. B **7**, 1521 (1990).
[11]T. Kobayashi and Y. Kida, Phys. Chem. Chem. Phys. **14**, 6200 (2012).
[12]A. H. Zewail, J. Phys. Chem. A **104**, 5660 (2000).
[13]V. Sundström, Phys. Chem. **59**, 53 (2008).
[14]S. B. van der Geer, O. J. Luiten, M. J. de Loos, G. Poeplau, and U. van Rienen, "3D space-charge model for GPT simulations of high brightness electron bunches," in *Institute of Physics Conference Series No. 175* (Institute of Physics, Bristol, UK, 2005), p. 101.
[15]M. Gullans, G. Penn, J. S. Wurtele, and M. Zolotorev, Phys. Rev. Spec. Top. - Accel. Beams **11**, 060701 (2008).
[16]A. J. W. Reitsma, R. A. Cairns, R. Bingham, and D. A. Jaroszynski, Phys. Rev. Lett. **94**, 085004 (2005).
[17]T. Eichner, F. Gruener, S. Becker, M. Fuchs, D. Habs, R. Weingartner, U. Schramm, H. Backe, P. Kunz, and W. Lauth, Phys. Rev. Spec. Top. - Accel. Beams **10**, 082401 (2007).
[18]M. P. Anania, D. Clark, S. B. van der Geer, M. J. de Loos, R. Isaac, A. J. W. Reitsma, G. H. Welsh, S. M. Wiggins, and D. A. Jaroszynski, Proc. SPIE **7359**, 735916 (2009).
[19]M. R. Islam, E. Brunetti, R. P. Shanks, B. Ersfeld, R. C. Issac, S. Cipiccia, M. P. Anania, G. H. Welsh, S. M. Wiggins, A. Noble, R. A. Cairns, G. Raj, and D. A. Jaroszynski, "Near-threshold electron injection in the laser-plasma wakefield accelerator leading to femtosecond bunches," Nature Physics (unpublished).
[20]O. Lundh, J. Lim, C. Rechatin, L. Ammoura, A. Ben-Ismaïl, X. Davoine, G. Gallot, J.-P. Goddet, E. Lefebvre, V. Malka, and J. Faure, Nat. Phys. **7**, 219 (2011).
[21]S. M. Wiggins, R. C. Issac, G. H. Welsh, E. Brunetti, R. P. Shanks, M. P. Anania, S. Cipiccia, G. G. Manahan, C. Aniculaesei, B. Ersfeld, M. R.

Islam, R. T. L. Burgess, G. Vieux, W. A. Gillespie, A. M. MacLeod, S. B. van der Geer, M. J. de Loos, and D. A. Jaroszynski, Plasma Phys. Controlled Fusion **52**, 124032 (2010).
[22]B. J. A. Shepherd and J. A. Clarke, Nucl. Instrum. Methods Phys. Res., Sect. A **654**, 8 (2011).
[23]J. G. Gallacher, M. P. Anania, E. Brunetti, F. Budde, A. Debus, B. Ersfeld, K. Haupt, M. R. Islam, O. Jaeckel, S. Pfotenhauer, A. J. W. Reitsma, E. G. Rohwer, H.-P. Schlenvoigt, H. Schwoerer, R. P. Shanks, S. M. Wiggins, and D. A. Jaroszynski, Phys. Plasmas **16**, 093102 (2009).
[24]N. D. Powers, I. Ghebregziabher, G. Golovin, C. Liu, S. Chen, S. Banerjee, J. Zhang, and D. P. Umstadter, Nat. Photonics **8**, 28 (2014).
[25]Z. He, J. A. Nees, B. Hou, B. Beaurepaire, V. Malka, K. M. Krushelnick, J. Faure, and A. G. R. Thomas, Proc. SPIE **8779**, 877905 (2013).
[26]G. Mourou, B. Brocklesby, T. Tajima, and J. Limpert, Nat. Photonics **7**, 258 (2013).
[27]B. W. J. McNeil, G. R. M. Robb, and D. A. Jaroszynski, Opt. Commun. **165**, 65 (1999).
[28]D. A. Jaroszynski, R. J. Bakker, A. F. G. van der Meer, D. Oepts, and P. W. Amersfoort, Phys. Rev. Lett. **71**, 3798 (1993).
[29]S. M. Wiggins, D. A. Jaroszynski, B. W. J. McNeil, G. R. M. Robb, P. Aitken, A. D. R. Phelps, A. W. Cross, K. Ronald, N. S. Ginzburg, V. G. Shpak, M. I. Yalandin, S. A. Shunailov, and M. R. Ulmaskulov, Phys. Rev. Lett. **84**, 2393 (2000).
[30]C. Lin, J. van Tilborg, K. Nakamura, A. J. Gonsalves, N. H. Matlis, T. Sokollik, S. Shiraishi, J. Osterhoff, C. Benedetti, C. B. Schroeder, Cs. Toth, E. Esarey, and W. P. Leemans, Phys. Rev. Lett. **108**, 094801 (2012).